Fungal Biology 123 (2019) 699–708

Contents lists available at ScienceDirect

Fungal Biology

journal homepage: www.elsevier.com/locate/funbio

Polysaccharide diversity in VNI isolates of *Cryptococcus neoformans* from Roraima, Northern Brazil

Halan D. Dal Pupo [a], Bianca A.G. Sena [b], Flavia C.G. Reis [b, c], Lumena Machado [d], Silvana T. Fortes [e], João N. de Almeida Junior [d, f], Rodrigo M.C. Godinho [g, 1], Marcio L. Rodrigues [b, g, *, 1]

[a] Programa de Pós-Graduação em Biologia Parasitária, Instituto Oswaldo Cruz, Fundação Oswaldo Cruz (Fiocruz), Rio de Janeiro, Brazil
[b] Instituto Carlos Chagas, Fiocruz, Curitiba, Brazil
[c] Centro de Desenvolvimento Tecnológico em Saúde (CDTS), Fundação Oswaldo Cruz, Rio de Janeiro, Brazil
[d] Laboratório de Micologia Médica, Instituto de Medicina Tropical, Universidade de São Paulo (USP), São Paulo, Brazil
[e] Laboratório de Micologia, Centro de Estudos da Biodiversidade, Universidade Federal de Roraima (UFRR), Roraima, Brazil
[f] Hospital Central da Faculdade de Medicina da Universidade de São Paulo (USP), São Paulo, Brazil
[g] Instituto de Microbiologia Paulo de Góes (IMPG), Universidade Federal do Rio de Janeiro (UFRJ), Rio de Janeiro, Brazil

ARTICLE INFO

Article history:
Received 21 March 2019
Received in revised form
3 June 2019
Accepted 3 June 2019
Available online 12 June 2019

Corresponding Editor: Vito Valiante

Keywords:
Capsule
Cryptococcal diversity
Glucuronoxylomannan
Glycan heterogeneity

ABSTRACT

Species of the *Cryptococcus* genus comprise environmental, encapsulated fungal pathogens that cause lethal meningitis in immunosuppressed individuals. In humans, fungal uptake of hypocapsular *Cryptococcus* by macrophages was associated with high fungal burden in the cerebrospinal fluid and long-term patient survival. On the basis of the key role of the cryptococcal capsule in disease, we analyzed the diversity of capsular structures in 23 isolates from pigeon excreta collected in the cities of Boa Vista, Bonfim and Pacaraima, in the state of Roraima (Northern Brazil). All isolates were identified as *Cryptococcus neoformans* (VNI genotype) by MALDI-TOF mass spectrometry. Through a combination of fluorescence microscopy, flow cytometry, ELISA and spectrophotometric methods, each isolate was characterized at the phenotypical level, which included measurements of growth rates at 30 and 37 °C, pigmentation, cell body size, capsular dimensions, serological reactivity, urease production and ability to produce extracellular glucuronoxylomannan (GXM), the main capsular component of *C. neoformans*. With the exception of melanization, a formidable diversity was observed considering all parameters tested in our study. Of note, hyper and hypo producers of GXM were identified, in addition to isolates with hyper and hypo profiles of reactivity with a polysaccharide-binding monoclonal antibody. Capsular dimensions were also highly variable in the collection of isolates. Extracellular GXM production correlated positively with capsular dimensions, urease activity and cell size. Unexpectedly, GXM concentrations did not correlate with serological reactivity with the cryptococcal capsule. These results reveal a high diversity in the ability of environmental *C. neoformans* to produce capsular components, which might impact the outcome of human cryptococcosis.

1. Introduction

The clinical syndromes caused by members of the *Cryptococcus* genus are responsible for approximately 200,000 deaths of humans each year (Rajasingham et al., 2017). The most lethal species in the genus is *Cryptococcus neoformans*. This fungus belongs to the VNI cryptococcal genotype and is part of the *Cryptococcus gattii/C. neoformans* species complex, which includes at least seven species (Hagen et al., 2015). Treatment of cryptococcosis is inefficient, toxic and expensive (Rodrigues, 2018), which points to the need of a better knowledge on the biology of *Cryptococcus*, aiming at the future design of novel therapeutic protocols.

Pathogenic species of the *C. gattii/C. neoformans* species complex are distributed in the environment. *C. gattii*, *Cryptococcus bacillisporus*, *Cryptococcus deuterogattii*, *Cryptococcus tetragattii*, *and*

* Corresponding author. Rua Professor Algacyr Munhoz Mader, 2135-2261-Cidade Industrial de Curitiba, Curitiba, PR, 81310-020, Brazil.
E-mail address: marcio.rodrigues@fiocruz.br (M.L. Rodrigues).
[1] RMCG and MLR share senior authorship on this manuscript.

https://doi.org/10.1016/j.funbio.2019.06.003
1878-6146/

Cryptococcus decagattii are usually associated with decayed hollows of mature trees, while *C. neoformans* and *Cryptococcus deneoformans* are common components of the microbial population of tropical soils and pigeon excreta (Kwon-Chung et al., 2015). Cryptococcal disease starts with inhalation of environmental spores or desiccated yeast and the outcome of the infection depends on multiple factors (Azevedo et al., 2016). Importantly, disease progress is directly impacted by the ability of cryptococci to cause damage to the host and/or to evade the immunological response (Dutra et al., 2018).

Members of the *C. gattii/C. neoformans* species complex are known for their ability to produce massive amounts of capsular polysaccharides (O'Meara and Andrew Alspaugh, 2012). The major capsular component of the complex is a heteropolysaccharide known as glucuronoxylomannan (GXM), an α1-3 mannan substituted with glucuronyl and xylosyl units. GXM, which accounts for approximately 90 % of the capsular mass, is believed to be constitutively produced by *Cryptococcus* both during laboratory cultivation and human/animal infections (O'Meara and Andrew Alspaugh, 2012). In fact, the most efficient methods of diagnosis of cryptococcosis are based on the serological detection of GXM in body fluids, implying that structural and serological differences may impact laboratory diagnosis. For capsule construction, GXM is synthesized in the intracellular environment, exported to the extracellular milieu and incorporated into the cell surface (Frases et al., 2009; Nimrichter et al., 2007).

Classification of members of the *Cryptococcus* genus was based on the serological reactivity of GXM during decades. However, it is now well known that serological classification is a minimalist criterion. For instance, analysis of cryptococcal isolates belonging to the same capsular serotype revealed important differences in the profile of reactivity of capsular polysaccharides with a panel of monoclonal antibodies, which illustrates the limitation of the serological classification of *Cryptococcus* (Rodrigues et al., 2015). However, cryptococcal polysaccharides directly impact disease progress. In animal models, it has been known for decades that GXM synthesis and capsule construction are required for cryptococcal virulence (O'Meara and Andrew Alspaugh, 2012). In humans, fungal uptake of hypocapsular *Cryptococcus* by macrophages was associated with high fungal burden in cerebrospinal fluid and long-term patient survival in human infections (Sabiiti et al., 2014).

Cryptococcosis due to VNI *C. neoformans* is endemic in the North region of Brazil. In the Amazon state, for instance, HIV-positive individuals were reported to be exclusively affected by VNI strains of *C. neoformans* (Fernando Silva Rocha et al., 2018). There is no reported information on the diversity in GXM production and serological reactivity in VNI isolates of *C. neoformans*. In this study, we monitored the presence of *C. neoformans* in samples of pigeon excreta in different sites of the city of Boa Vista (Roraima state, North Brazil) and adjacencies. We identified 23 isolates as *C. neoformans* VNI. Phenotypical analysis of this isolate collection revealed important differences in a number of parameters related to GXM and other properties, suggesting a high diversity in polysaccharide production and a still unpredictable impact on human disease.

2. Methods

2.1. Isolation and identification of microorganisms

In all assays, the standard VNI strain H99 of *C. neoformans* was used as a reference isolate. Environmental samples (n = 212) were collected in three different cities of the Roraima state, including its capital (Boa Vista; n = 184) and two frontier cities, namely Pacaraima (border with Venezuela; n = 8) and Bonfim (border with the Co-operative Republic of Guyana, n = 20). The samples were collected from November 2016 to January 2017 from random, public places that included high daily people flow. Six additional isolates obtained earlier from pigeon droppings in the city of Boa Vista (RR2605, collected in 1997; Pb isolates, obtained in 2002; see Table 1 for details) were also included in the present study. These isolates were kept in skin milk at −20 °C in the Mycology Laboratory (Biodiversity Research Center, Federal University of Roraima, UFRR) before transfer to Niger seed agar or solid Sabouraud medium for regular cultivation. Bird droppings (1 g) were first macerated and suspended in 10 ml of sterile saline solution supplemented with 5 mg/ml gentamicin. Part of this suspension (100 μl) was plated on Niger seed agar (Staib, 1962) supplemented with 0.2 mg/ml chloramphenicol. The plates were cultivated for 7 d at 37 °C and melanization was assessed visually. Dark brown colonies were selected for microscopic examination. Those manifesting the typical features of *Cryptococcus* spp (round-oval budding yeast cells) were individually transferred to Sabouraud dextrose agar for further identification by matrix-assisted laser desorption/ionization time-of-flight mass spectrometry (MALDI-TOF MS) as described below. Maps with the collection sites from which positive hits were obtained are summarized in Fig. 1.

2.2. MALDI-TOF MS analysis

Protein extraction from each isolate was performed through the transfer of one loop of yeast biomass to a 1.5-ml microcentrifuge tube containing 300 μl of purified water. The suspension was mixed with 900 μl of ethanol and the samples were spin-centrifuged. Sediments were vacuum dried and further suspended in 50 μl of 70 % formic acid. An equivalent volume of acetonitrile was added, and the mixture was again centrifuged. Supernatant samples (1 μl, quadruplicates) was spotted onto a disposable MALDI target slide composed of a polypropylene carrier with a stainless-steel layer (bioMérieux). After air-drying, each spot was overlaid with 1 μl of α-cyano-4-hydroxycinnamic acid (HCCA) matrix (bioMérieux). Samples were analyzed on a Vitek MS instrument (bioMérieux) and the spectra were generated using the Launchpad version 2.8 software (bioMérieux). Data analysis was performed with the Saramis Premium software (version 4.12, bioMérieux). Genotype identification was based on a recent study using MALDI-TOF MS to discriminate between cryptococcal genotypes (Siqueira et al., 2019).

2.3. Spectrophotometric determination of growth rates and urease activity

All strains were cultivated overnight in liquid Sabouraud medium as described before. The cells were washed twice in phosphate-buffered saline (PBS), adjusted to an optical density (λ = 600) of 0.01 and incubated at 30 or 37 °C in the same medium under shaking (200 rpm). Aliquots of each cultures were taken at 4, 6, 8, 10, 12, 24 and 48 h for optical density assessment. For determination of urease activity, the cells were grown for 24 h in liquid Sabouraud medium, washed three times with PBS and tested as described before (Rodrigues et al., 2008).

2.4. Microscopic and immunofluorescence analyses

Yeast cells were cultivated in liquid Sabouraud medium for 16 h at 30 °C under shaking (200 rpm). The cells were then washed twice in PBS and incubated in a chemically defined minimal medium composed of glucose (15 mM), $MgSO_4$ (10 mM), KH_2PO_4 (29.4 mM), glycine (13 mM), and thiamine-HCl (3 μM), pH 5.5, for 3 d under the same conditions described above. The cells were

Table 1
MALDI-TOF MS identification of *C. neoformans* in the state of Roraima, Northern Brazil[a].

Isolate	Species	Genotype	Confidence level identification (%)	Identification Score (range)
1B	*C. neoformans*	VNI	99,90 %	1224
2B	*C. neoformans*	VNI	99,90 %	1235
2C	*C. neoformans*	VNI	99,90 %	1235
2D	*C. neoformans*	VNI	99,90 %	1240
4C	*C. neoformans*	VNI	99,90 %	1245
7	*C. neoformans*	VNI	99,90 %	1225
33A1	*C. neoformans*	VNI	99,90 %	1221
54A1	*C. neoformans*	VNI	99,90 %	1237
56A1	*C. neoformans*	VNI	99,90 %	1250
68B1	*C. neoformans*	VNI	99,90 %	1250
69A1	*C. neoformans*	VNI	99,90 %	1246
81A1	*C. neoformans*	VNI	99,90 %	1250
96A1	*C. neoformans*	VNI	99,90 %	1230
106A1	*C. neoformans*	VNI	99,90 %	1243
144A1	*C. neoformans*	VNI	99,90 %	1242
151A1	*C. neoformans*	VNI	99,90 %	1235
176A1	*C. neoformans*	VNI	99,90 %	1232
3Pb3	*C. neoformans*	VNI	99,90 %	1368
5Pb2	*C. neoformans*	VNI	99,90 %	1249
19Pb4	*C. neoformans*	VNI	99,90 %	1158
23Pb2	*C. neoformans*	VNI	99.90 %	1221
32Bp1	*C. neoformans*	VNI	99,90 %	1235
RR 2605	*C. neoformans*	VNI	99,90 %	1236

[a] Fungal identification was based on the data provided by the SARAMIS Premium software (bioMérieux) with a validated in-house database of *C. neoformans* and *C. gattii* genotypes spectral profiles (Siqueira et al., 2019). Score values above 1000 points correlate with a 99.9 % confidence level of identification. None of the isolates had scores above 1000 points for other genotypes.

harvested by centrifugation, washed in PBS and fixed in 4 % paraformaldehyde (1 h at room temperature). The cells were further blocked with 1 % bovine serum albumin (BSA) in PBS (1 h, 37 °C) and incubated with the monoclonal IgG1 18B7 (mAb 18B7; 10 μg/ml, 1 h, 37 °C). Mab18B7 is a monoclonal antibody (mAb) raised against GXM that was kindly donated by Dr. Arturo Casadevall (Johns Hopkins University). After washing, the cells were subsequently incubated with an Alexa Fluor 488-conjugated secondary antibody (10 μg/ml, 1 h, 37 °C; Invitrogen, USA). The cells were also stained with calcofluor white (5 μg/ml, 1 h, 37 °C; Invitrogen, USA) for cell wall visualization. The cells were again washed with PBS and counterstained with India ink for capsular measurement. All images were acquired using a fluorescence optical microscope Axioplan 2 (Zeiss, Germany) with a 63X immersion objective. For quantitative determination of cellular dimensions, cell and capsular diameters were determined in India ink counterstained cells (n = 100) using the Fiji software. Capsular dimensions were expressed as the ratio between capsular and cell diameters, while cell diameters were expressed in μm and denominated cell body measurements to avoid confusion with capsular dimensions.

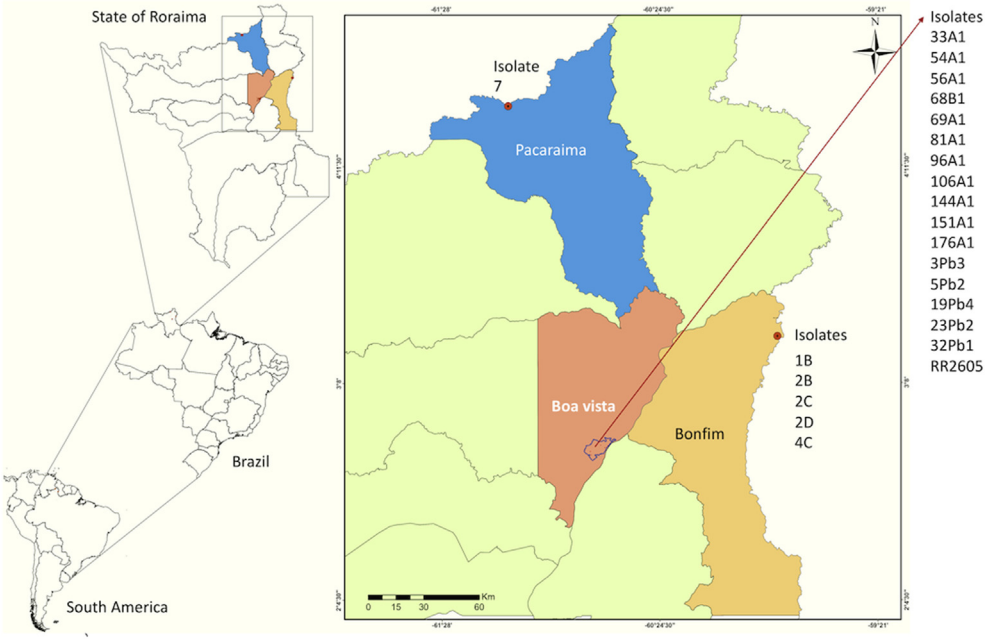

Fig. 1. Geographical illustration of the sites of collection of identified *C. neoformans* samples. The cities where positive hits were identified (Pacaraima, Boa Vista and Bonfim) are highlighted. Corresponding isolates are adjacent to the source cities (Pacaraima and Bonfim; 1 and 5 isolates, respectively) or listed on the right side of the map (Boa Vista; 17 isolates).

2.5. Detection of surface-associated and extracellular GXM

Fungal cells were cultivated in YPD (yeast extract-peptone-dextrose) for 48 h at 30 °C and transferred to RPMI, for further incubation for 24 h at 37 °C for induction of GXM secretion (O'Meara and Andrew Alspaugh, 2012). Fungal cells were collected and prepared for staining with mAb 18B7 as described above for immunofluorescence analysis. The cells were analyzed with a FACS Canto II flow cytometer as recently described by our group (Reis et al., 2019). Data was processed with the FACSDiva Version software, version 6.1.3. The reactivity of each culture supernatant with mAb 18B7 was determined by ELISA as previously described (Casadevall et al., 1992). Briefly, supernatants were collected by centrifugation and used to coat the wells of a 96-well polystyrene plate. After removal of unbound molecules, the plates were blocked with 1 % bovine serum albumin and a solution of mAb 18B7 was added to the plates, followed by incubation for 1 h at 37 °C. The plates were washed and incubated with an alkaline phosphatase-conjugated goat anti-mouse IgG1 for 1 h at 37 °C. Reactions were developed after the addition of p-nitrophenyl phosphate disodium hexahydrate, followed by spectrophotometric reading at 405 nm. Standard solutions of GXM prepared after polysaccharide aggregation by ultrafiltration of supernatants (Nimrichter et al., 2007) were used for elaboration of standard curves and GXM quantification in supernatant fractions.

2.6. Statistical analyses

Statistical analyses were performed with the GraphPad software (La Jolla, CA). Group comparisons were submitted to multiple comparison analysis of variance (ANOVA) and paired comparisons were performed with the Student's *t* test. Correlation tests were also performed with the GraphPad software for calculation of R squared and P values. Significant values of correlation were defined using the 0.05 cutoff. Collection of data for correlation analyses included average values of supernatant GXM (μg/ml), extracellular urease (absorbance units), cell body diameters (μm), capsule size (μm), and serological reactivity of the capsule with mAb 18B7 (fluorescence units obtained from flow cytometry analysis) of 24 XY pairs (23 isolates plus the standard strain H99).

3. Results

3.1. Identification of C. neoformans in environmental samples

Due to the clinical importance of VNI *C. neoformans* in the Northern region of Brazil (Fernando Silva Rocha et al., 2018) and its association with pigeon excreta (Kwon-Chung et al., 2015), the samples selected for our study were limited to bird droppings. MALDI-TOF MS of isolated cultures demonstrated that all positive hits corresponded to VNI *C. neoformans* (Table 1). Positivity identification rates in the dropping samples corresponded to 25 % in samples obtained in city of Bonfim (5 out of 20 isolates), 12.5 % in Pacaraima (1 out of 8 isolates) and 6 % in the state capital Boa Vista (11 out of 184 isolates).

3.2. Phenotypic characterization of the C. neoformans isolates

Melanin is a major virulence factor in the *Cryptococcus* genus (Kwon-Chung et al., 2015), which led us to evaluate whether the isolates identified as VNI *C. neoformans* would have different kinetics of melanization. The 23 isolates had similar pigmentation potential after cultivation in Niger seed agar (Fig. 2). Since proliferation rates at 30 and 37 °C are directly linked to the ability of *C. neoformans* to survive in the environment and in the host, respectively, we determined the ability of all isolates to grow at each temperature (Fig. 3). Eight isolates grew faster at the first 12 h, but no differences between all isolates were observed after 24 h of cultivation. The only exception was isolate 3Pb3, which clear showed lower proliferation rates after 12 and 24 h of cultivation. Due to the well-known role of urease in cryptococcal pathogenesis (Kwon-Chung et al., 2015), this enzyme's extracellular activity was also determined (Fig. 4). Most isolates manifested levels of urease activity that were similar to that found in the standard isolate H99. However, 8 isolates (56A1, 81A1, 106A1, 176A1, 5Pb2, 19Pb4, RR2605 and 23Pb2) produced much lower enzyme activity.

3.3. Polysaccharide diversity in the C. neoformans isolates

All isolates were processed for microscopic examination by India ink counterstaining and surface analysis by fluorescence microscopy (Fig. 5). Although all of them corresponded to VNI *C. neoformans*, a great morphological variation was observed after India ink counterstaining. Visual analysis of capsule size revealed very small (see isolate 56A1 in Fig. 5, for illustration), moderately reduced (see isolate RR2605 in Fig. 5, for illustration) and large (see isolate 2D in Fig. 5, for illustration) capsular dimensions. Differences in the cell diameters were also apparent, as concluded from the detection of very small cells (see isolate 106A1 in Fig. 5, for illustration), yeast cells with the typical cryptococcal dimensions (most isolates, see isolate 3Pb3 in Fig. 5 for illustration) and one isolate (151A1, Fig. 5) with diameter values that were compatible with those described for Titan cells. Differences in chitin content were also suggested, as inferred from the reduced reactivity of isolates 5Pb2, 19Pb4 and 176A1 with calcofluor white (Fig. 5).

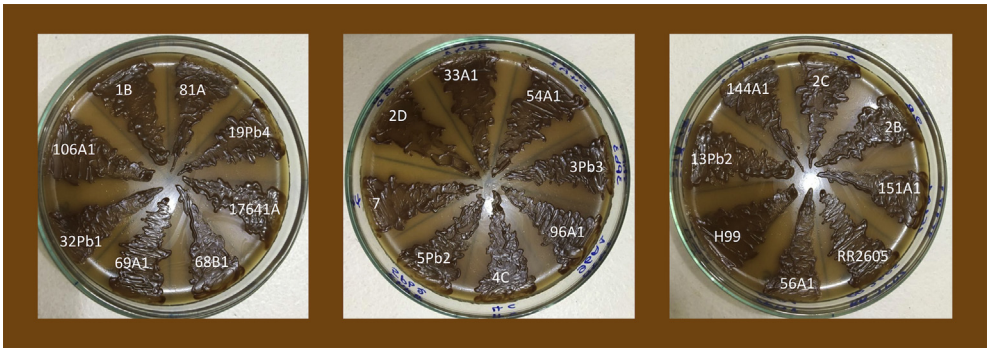

Fig. 2. Melanization of VNI *C. neoformans* isolates on Niger seed agar. No visual differences were observed between any of the *C. neoformans* cultures. Results in all panels are representative of three independent experiments.

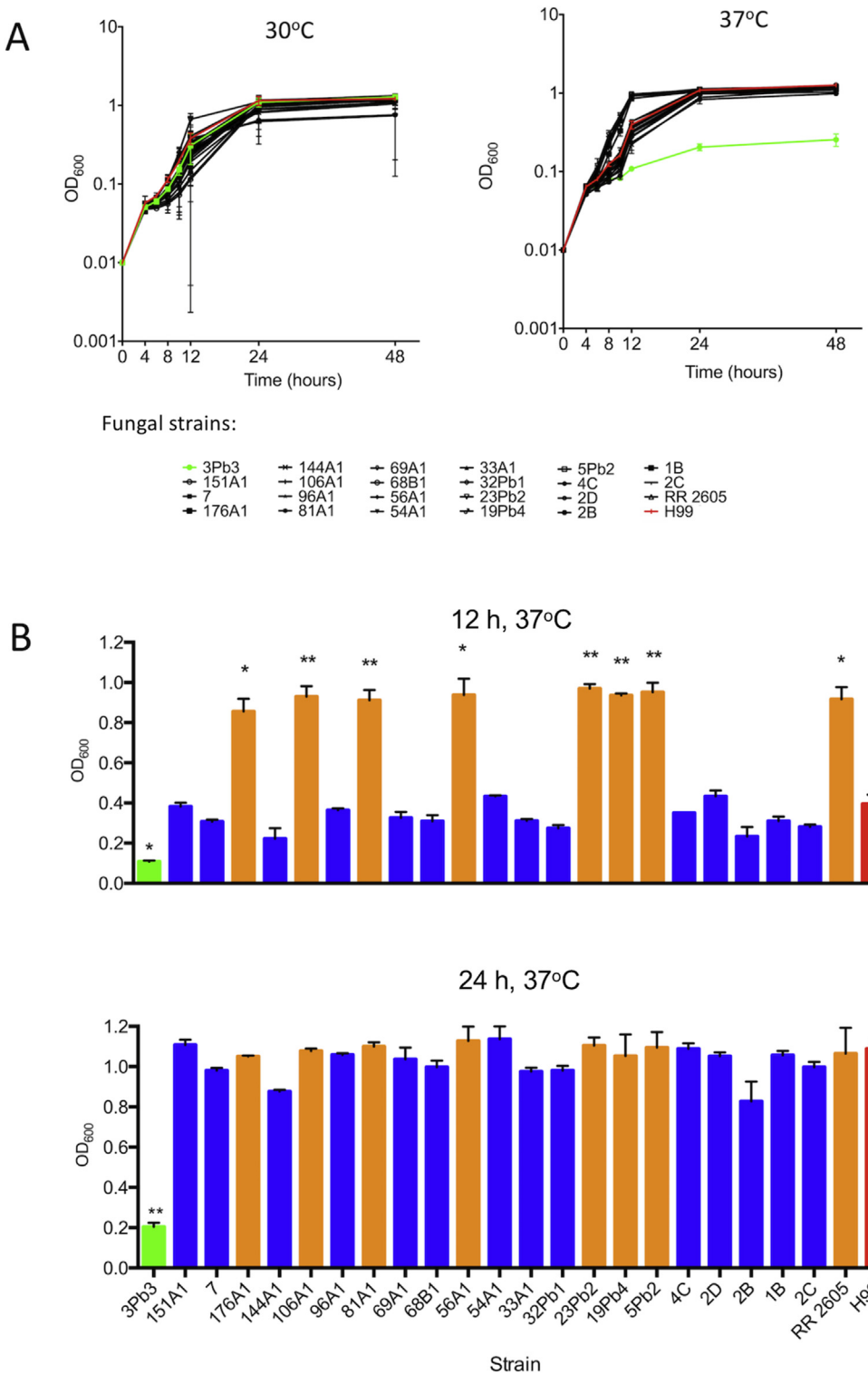

Fig. 3. Growth rates of the 23 *C. neoformans* isolates from the state of Roraima, Brazil, in comparison with the standard strain H99. (A). Spectrophotometric measurement of the growth of each isolate tested at 30 (left panel) and 37 °C (right panel). The standard strain H99 is highlighted in red. All isolates had similar growth rates, excepting isolate 3Pb3, which manifested lower ability to proliferate at 37 °C (green line). (B). Statistical analysis of proliferation rates at 12 and 24 h after inoculation in culture medium. Orange bars denote altered fungal growth after 12 h (*P < 0.05; **P < 0.0001) in comparison to strain H99 (red bar). Blue bars denote fungal growth at rates that were similar to that described for strain H99. After 24 h, only isolate 3Pb3 (green bar) had proliferation rates that were statistically different from that calculated for strain H99. Growth determinations are representative of three independent experiments. (For interpretation of the references to color in this figure legend, the reader is referred to the Web version of this article.)

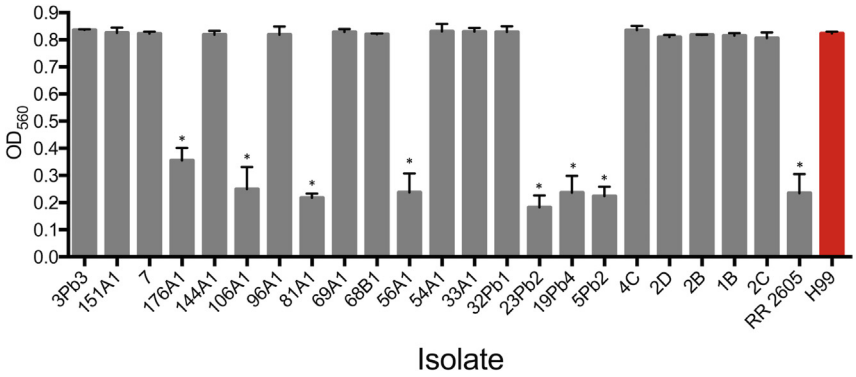

Fig. 4. Determination of urease activity in culture supernatants of the *C. neoformans* isolates from Roraima, in comparison to strain H99. With the exception of isolates 176A1, 106A1, 81A1, 56A1, 23Pb2, 19Pb4, 5Pb2, and RR2605, which produced significantly lower levels of urease activity in comparison to strain H99 (asterisks, $P < 0.0001$), all isolates produced similar levels of urease activity. Results are representative of three independent experiments.

Capsular reactivity with mAb 18B7 revealed at least three different profiles of antibody-based capsule staining (Fig. 5), which we classified as annular, punctuate and surface dotted. Virtually negative serological reactions were also observed. Most isolates ($n = 11$) belonged to the punctuate classification (isolates 3Pb3, 7, 144A1, 96A1, 69A1, 68B1, 54A1, 33A1, 2B, 2C and 2D), while three isolates gave undetectable fluorescence (176A1, 106A1 and 5Pb2). Five isolates manifested the annular pattern (151A1, 81A1, 32Pb1, 4C and 1B) and four isolates showed surface fluorescence dots (56A1, 23Pb2, 19Pb4 and RR22605). Considering that all isolates supposedly belong to the same serotype, these results pointed to the limitations of the serotype-based classification of *Cryptococcus*.

The visual perception that capsular and cell body dimensions were variable were confirmed by quantitative determinations (Fig. 6). Cell diameters varied from 1 to 30 μm in the whole isolate collection, with average values most concentrated in the 7–8 μm range (Fig. 6A). Most strikingly, cell diameter varied from 2 to 30 μm in isolate 151A1, the one reaching the highest dimensions. Isolates 23PB2, 19PB4, 5PB2 and RR2605, on the other hand, had the lowest average values of cell diameter (approximately 2 μm). Capsular dimensions were expressed as the ratio between capsule and cell diameters (Fig. 6B). Therefore, smaller capsules generated values closer to 1 and larger capsules produced higher values. Average values varied from approximately 1.4 to 2.2, with isolate 2D manifesting the largest capsule.

The *C. neoformans* isolates were also analyzed under conditions of GXM secretion and capsule induction (24 h incubation in RPMI, 37 °C). Indeed, the reactivity of the 23 *C. neoformans* isolates with mAb 18B7 was increased, as quantified by flow cytometry (Fig. 7). GXM release to the extracellular space is required for capsule construction and immune modulation (Nimrichter et al., 2007; Rodrigues et al., 2007). Therefore, on the basis of the importance of extracellular GXM for both physiology and pathogenesis, we analyzed the reactivity of extracellular polysaccharides produced by each isolate with mAb 18B7 and compared to the standard isolate H99 (Fig. 8). Once again, a great diversity between the different isolates was observed. Based on antibody reactivity, extracellular GXM concentrations were determined, producing variations from 1 to approximately 30 μg/ml.

3.4. Correlation analysis of cellular dimensions, capsule size, detection of extracellular GXM, serological recognition of the cell surface and urease activity

After the collection of information on a number of different parameters, we performed a multifactorial analysis of the major phenotypic features observed in the *C. neoformans* collection. We analyzed the mathematical correlation between capsule size, cellular diameters, urease activity, extracellular GXM detection and serological reactivity of mAb 18B7 with the cryptococcal capsule

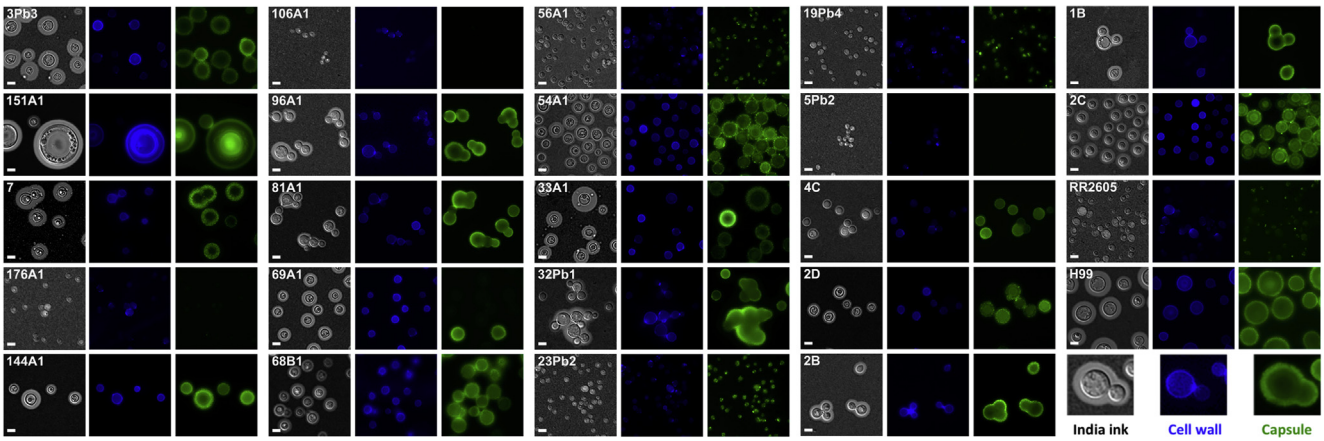

Fig. 5. Microscopic examination of the *C. neoformans* isolates from Roraima and the standard strain H99. For each isolate, India ink counterstaining (dark field panels), calcofluor white binding (blue fluorescence) and GXM staining (green fluorescence) are shown. See bottom, right panel for illustration of the cellular compartments analyzed. Scale bars, 5 μm. (For interpretation of the references to color in this figure legend, the reader is referred to the Web version of this article.)

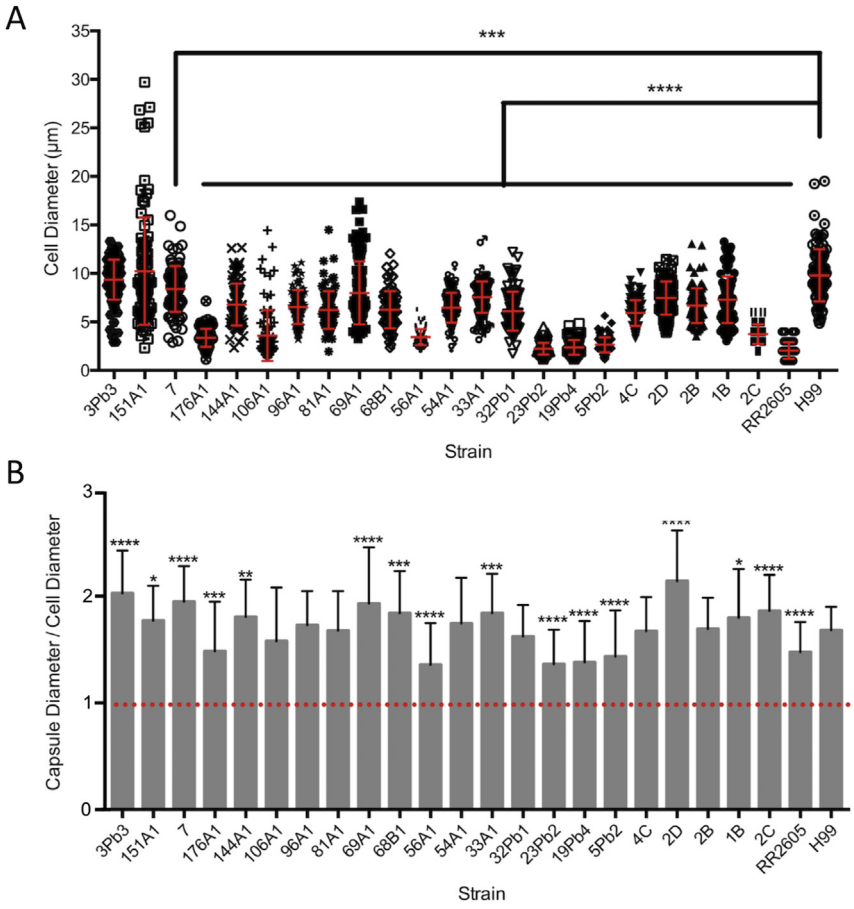

Fig. 6. Quantitative determination of cellular dimensions in the *C. neoformans* environmental isolates in comparison to strain H99. (A). Cell diameter analysis. Statistical differences resulting from cell diameter analysis in comparison to strain H99 are highlighted with asterisks (***P = 0.0001 and ****P < 0.0001). (B). Capsular/cellular diameter ratios. Statistical differences in comparison to strain H99 are highlighted with asterisks (*P < 0.05; **P < 0.005; ***P < 0.0005 and ****P < 0.0001). Results are representative of three independent experiments.

(Fig. 9). A strong correlation between capsule size and cell body dimensions was observed (P < 0.0001). Cellular dimensions were also correlated with urease activity (P < 0.0001) and detection of extracellular GXM (P = 0.0034), but not with serological reactivity of mAb 18B7 with the capsule (P = 0.4578). In addition to correlating with cellular dimensions, capsule size correlated with urease activity (P < 0.0001) and GXM detection (P = 0.0032), but not with mAb18B7 binding to the capsule (P = 0.6837). Urease activity was also correlated with extracellular GXM detection (P = 0.0273). Negative results were observed when antibody binding was correlated with capsular dimensions (P = 0.4425) and with urease activity (P = 0.7258).

4. Discussion

Fungal species causing disease in humans and animals are mostly represented by environmental microbes that developed mechanisms to cause damage to mammalian hosts (Camacho and Casadevall, 2018). In this context, it is now clear that the virulence arsenal used by fungal cells during disease, including the cryptococcal capsule, is impacted by the environment (de Araujo et al., 2012). Therefore, the potential for pathogenic diversity in environmental strains and the consequent impact in human diseases is still unpredictable. In our study we analyzed the phenotypic features of *C. neoformans* environmental isolates obtained from an endemic region of Brazil. In these isolates, we observed considerable diversity in a number of parameters. However, the most striking differences were related to urease, a major virulence factor required for brain invasion, and components of the cryptococcal capsule, which is supposedly required for persistence of *C. neoformans* in the mammalian host (O'Meara and Andrew Alspaugh, 2012).

The analysis of the pathogenesis-related characteristics of each isolate revealed a high complexity. For instance, it is well known that capsule formation, GXM release and urease production are all essential for cryptococcal virulence (Kwon-Chung et al., 2015). Several isolates were efficient in producing all of the three virulence determinants. Other isolates, on the other hand, produced more complex phenotypic panels. Isolate 3Pb3, for instance, was the highest producer of extracellular GXM. This isolate was also efficient in forming a capsule and produced high urease levels but had defective growth at 37 °C. Isolates 23Pb2, 19Pb4, and 5Pb2 grew well at 37 °C, but were low producers of capsule, urease and extracellular GXM. Other isolates (4C, for instance) were efficient producers of all factors analyzed in our study. In this context, it seems unlikely that fungal isolates with defective growth at 37 °C will have relevant pathogenic potential even under conditions of high urease and GXM production. Similarly, fast growing strains would likely fail to cause damage to the host under conditions of reduced expression of virulence factors. In summary, these results suggest that the pathogenic potential of the environmental isolates of Roraima is hard to predict, but highly diverse.

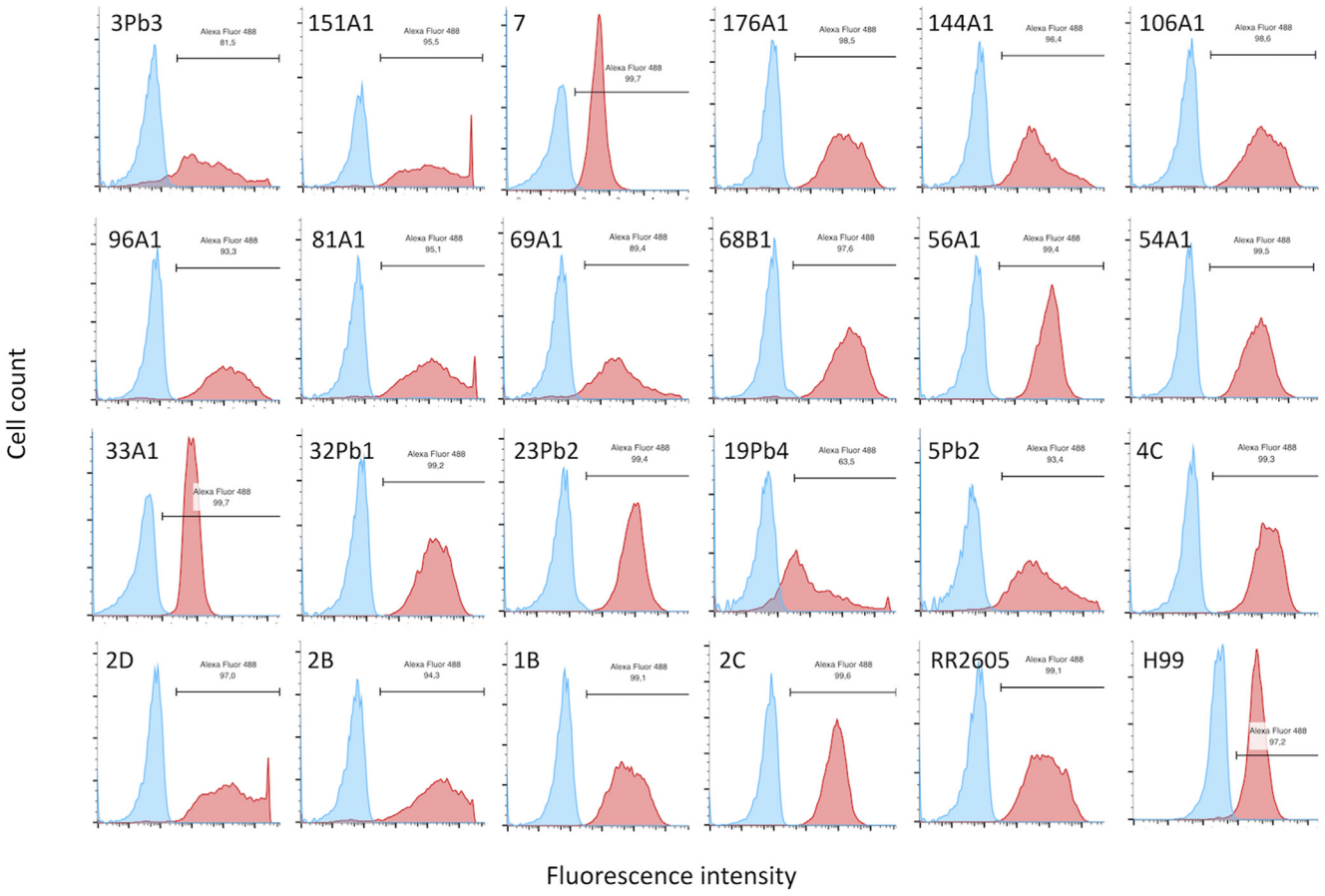

Fig. 7. Quantitative determination of the reactivity of mAb 18B7 with the *C. neoformans isolates*. Flow cytometry analysis is shown for each isolate. Blue histograms represent negative controls (no primary antibody). Red histograms represent staining of fungal cells with mAb 18B7. Results in all panels are representative of two independent experiments. (For interpretation of the references to color in this figure legend, the reader is referred to the Web version of this article.)

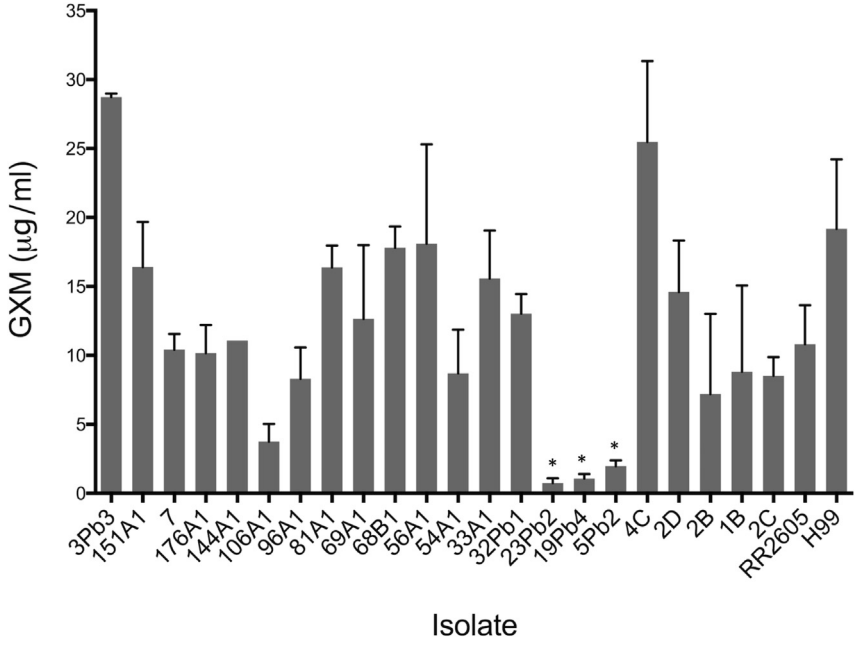

Fig. 8. Extracellular GXM detection by ELISA. Each supernatant was analyzed for reactivity with mAb 18B7, which demonstrated profiles of low (isolates 106A1, 23Pb2, 19Pb4, 5Pb2), intermediate (isolates 151A1, 7, 176A1, 144A1, 96A1, 81A1, 69A1, 68B1, 56A1, 54A1, 33A1, 32Pb1, 2D, 2B, 1B, 2C and RR2605) and high (3Pb3 and 4C) detection of GXM through reactivity with mAb 18B7. Statistical analysis revealed significant differences (asterisks, $P < 0.05$) only when three of the four lower polysaccharide producers (23Pb2, 19Pb4, 5Pb2) where compared to the most efficient producers of GXM (isolates 3Pb3, 4C and the standard strain H99). Results are representative of four independent experiments.

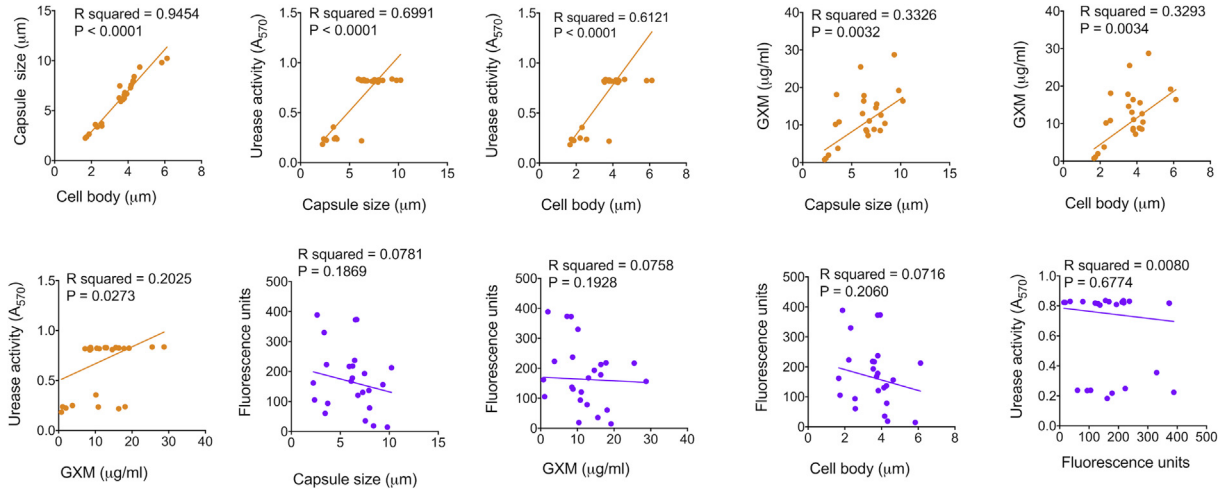

Fig. 9. Correlation analyses of the different parameters measured in the current study. Correlation panels start with highest correlation values, as inferred from the calculation of R squared values and statistical significance (P values). Orange lines/dots denote positive correlation; purple lines/dots denote no correlation. (For interpretation of the references to color in this figure legend, the reader is referred to the Web version of this article.)

All isolates used in our study belonged to the VNI genotype of *C. neoformans*, which corresponds to the variety *grubii* according to the traditionally used classification system of the *C. neoformans/C. gattii* species complex (Hagen et al., 2015). *C. neoformans* var. *grubii* produces serotype A capsular polysaccharides (Zaragoza et al., 2009). Polysaccharide serotyping is based on the relationship between serological recognition and structural particularities (Kwon-Chung et al., 2015), which implies that VNI isolates are expected to produce similar patterns of antibody recognition. Our current results strongly contradict this assumption, as concluded from the variable patterns of serological recognition of the isolates by mAb 18B7. This observation likely impacts the interpretation of our model of GXM detection in culture supernatants. Extracellular GXM reactivity with mAb 18B7 was highly variable, which could certainly be resultant from differential abilities of each isolate to produce and export GXM. However, our immunofluorescence analysis revealed that the *C. neoformans* isolates had different profiles of antibody reactivity. Therefore, it is indeed possible that the collection of isolates analyzed in this study comprises low, medium and high producers of GXM. However, the possibility that different structures of GXM are produced in the isolate collection cannot be ruled out. Besides confirming the prevalence of these isolates in Northern Brazil (Fernando Silva Rocha et al., 2018), these results efficiently illustrated the limitations of the serotype-based classification.

Our study revealed interesting and still poorly understood correlations between different phenotypic features in *C. neoformans*. Some of the positive correlations were in fact expected (capsule size or cellular dimensions with extracellular GXM detection). In fact, the strongest correlation observed in our study resulted from the analysis of capsular and cellular dimensions. However, we also observed puzzling correlation values involving urease activity, which correlated with cellular dimensions, capsule size and antibody-based detection of extracellular GXM. Secretory activity is mandatory for the functionality of all four parameters (Oliveira et al., 2013), which suggests a link between the secretory potential of each isolate with the ability to produce virulence mechanisms. On the other hand, serological recognition of the capsule did not correlate with directly linked properties of the *C. neoformans* biology, including capsule size and extracellular detection of GXM. Capsule recognition by mAb 18B7, in fact, did not correlate with any of the parameters analyzed in our study, confirming the above-discussed notion that capsular serological properties consist of a fragile system of classification in the *Cryptococcus* genus.

High fungal burden in the cerebrospinal fluid is an adverse prognostic marker of cryptococcosis (Colombo and Rodrigues, 2015). In fact, high fungal loads in the cerebrospinal fluid were correlated with high levels of fungal uptake by macrophages *in vitro* in a previous study (Sabiiti et al., 2014). Higher phagocytosis, on the other hand, was associated to a hypocapsular phenotype. This observation contradicts the notion that phagocytosis inhibition through enhanced capsular dimensions is beneficial for *C. neoformans*. The significance of the findings herein described for the pathogenic potential of *C. neoformans* still needs to be explored, but the high diversity observed in our study is compatible with the observation that phenotypic features can correlate with disease outcome.

Acknowledgements

We thank Arturo Casadevall for providing the antibody to GXM (MAb 18B7). We also thank Juliana Rizzo and Priscila Albuquerque for helpful advice to HDDP. M.L.R. is currently on leave from the position of Associate Professor at the Microbiology Institute of the Federal University of Rio de Janeiro, Brazil. This work was supported by grants from the Brazilian agency Conselho Nacional de Desenvolvimento Cientifico e Tecnologico (CNPq, grants 405520/2018-2, 440015/2018-9, and 301304/2017-3) and FIOCRUZ (grants VPPCB-007-FIO-18-2-57 and VPPIS-001-FIO-18-66) to MLR. We also acknowledge support from Coordenacao de Aperfeicoamento de Pessoal de Nivel Superior (CAPES, finance code 001) and the Instituto Nacional de Ciencia e Tecnologia de Inovacao em Doencas de Populacoes Negligenciadas (INCT-IDPN). We have no conflicts of interest to declare.

References

Azevedo, R., Rizzo, J., Rodrigues, M., 2016. Virulence factors as targets for anti-cryptococcal therapy. J. Fungi 2, 29. https://doi.org/10.3390/jof2040029.

Camacho, E., Casadevall, A., 2018. Cryptococcal traits mediating adherence to biotic and abiotic surfaces. J. Fungi. https://doi.org/10.3390/jof4030088.

Casadevall, A., Mukherjee, J., Scharff, M.D., 1992. Monoclonal antibody based ELISAs for cryptococcal polysaccharide. J. Immunol. Methods. https://doi.org/10.1016/0022-1759(92)90209-C.

Colombo, A.C., Rodrigues, M.L., 2015. Fungal colonization of the brain: anatomo-pathological aspects of neurological cryptococcosis. An. Acad. Bras. Cienc. 87, 1293–1309. https://doi.org/10.1590/0001-3765201520140704.

de Araujo, G.S., Fonseca, F.L., Pontes, B., Torres, A., Cordero, R.J.B., Zancopé-Oliveira, R.M., Casadevall, A., Viana, N.B., Nimrichter, L., Rodrigues, M.L., Garcia, E.S., de Souza, W., Frases, S., 2012. Capsules from pathogenic and non-pathogenic Cryptococcus spp. manifest significant differences in structure and ability to protect against phagocytic cells. PLoS One 7. https://doi.org/10.1371/journal.pone.0029561.

Dutra, F.F., Albuquerque, P.C., Rodrigues, M.L., Fonseca, F.L., 2018. Warfare and defense: the host response to Cryptococcus infection. Fungal Biol. Rev. 32, 35–51. https://doi.org/10.1016/j.fbr.2017.09.002.

Fernando Silva Rocha, D., Cruz, K.S., da Silva Santos, C.S., Stephanny Fernandes Menescal, L., da Silva Neto, J.R., Pinheiro, S.B., Silva, L.M., Trilles, L., Vicente Braga de Souza, J., 2018. MLST reveals a clonal population structure for *Cryptococcus neoformans* molecular type VNI isolates from clinical sources in Amazonas, Northern-Brazil. PLoS One. https://doi.org/10.1371/journal.pone.0197841.

Frases, S., Pontes, B., Nimrichter, L., Viana, N.B., Rodrigues, M.L., Casadevall, A., 2009. Capsule of *Cryptococcus neoformans* grows by enlargement of polysaccharide molecules. Proc. Natl. Acad. Sci. U. S. A. 106. https://doi.org/10.1073/pnas.0808995106.

Hagen, F., Khayhan, K., Theelen, B., Kolecka, A., Polacheck, I., Sionov, E., Falk, R., Parnmen, S., Lumbsch, H.T., Boekhout, T., 2015. Recognition of seven species in the Cryptococcus gattii/*Cryptococcus neoformans* species complex. Fungal Genet. Biol. https://doi.org/10.1016/j.fgb.2015.02.009.

Kwon-Chung, K.J., Fraser, J.A., Doering, T.Á.L., Wang, Z.A., Janbon, G., Idnurm, A., Bahn, Y.S., 2015. *Cryptococcus neoformans* and Cryptococcus gattii, the etiologic agents of cryptococcosis. Cold Spring Harb. Perspect. Med. https://doi.org/10.1101/cshperspect.a019760.

Nimrichter, L., Frases, S., Cinelli, L.P., Viana, N.B., Nakouzi, A., Travassos, L.R., Casadevall, A., Rodrigues, M.L., 2007. Self-aggregation of *Cryptococcus neoformans* capsular glucuronoxylomannan is dependent on divalent cations. Eukaryot. Cell 6. https://doi.org/10.1128/EC.00122-07.

O'Meara, T.R., Andrew Alspaugh, J., 2012. The *Cryptococcus neoformans* capsule: a sword and a shield. Clin. Microbiol. Rev. https://doi.org/10.1128/CMR.00001-12.

Oliveira, D.L., Rizzo, J., Joffe, L.S., Godinho, R.M.C., Rodrigues, M.L., 2013. Where do they come from and where do they go: candidates for regulating extracellular vesicle formation in fungi. Int. J. Mol. Sci. 14. https://doi.org/10.3390/ijms14059581.

Rajasingham, R., Smith, R.M., Park, B.J., Jarvis, J.N., Govender, N.P., Chiller, T.M., Denning, D.W., Loyse, A., Boulware, D.R., 2017. Global burden of disease of HIV-associated cryptococcal meningitis: an updated analysis. Lancet Infect. Dis. 17, 873–881. https://doi.org/10.1016/S1473-3099(17)30243-8.

Reis, F.C.G., Borges, B.S., Jozefowicz, L.J., Sena, B.A.G., Garcia, A.W.A., Medeiros, L.C., Martins, S.T., Honorato, L., Schrank, A., Vainstein, M.H., Kmetzsch, L., Nimrichter, L., Alves, L.R., Staats, C.C., Rodrigues, M.L., 2019. A novel protocol for the isolation of fungal extracellular vesicles reveals the participation of a putative scramblase in polysaccharide export and capsule construction in Cryptococcus gattii. mSphere 4 e00080-19. https://doi.org/10.1128/mSphere .00080-19.

Rodrigues, J., Fonseca, F.L., Schneider, R.O., Godinho, R.M.D.C., Firacative, C., Maszewska, K., Meyer, W., Schrank, A., Staats, C., Kmetzsch, L., Vainstein, M.H., Rodrigues, M.L., 2015. Pathogenic diversity amongst serotype C VGIII and VGIV Cryptococcus gattii isolates. Sci. Rep. 5, 11717. https://doi.org/10.1038/srep11717.

Rodrigues, M.L., 2018. Neglected disease, neglected populations: the fight against cryptococcus and cryptococcosis. Mem. Inst. Oswaldo Cruz 113, 7–8. https://doi.org/10.1590/0074-02760180111.

Rodrigues, M.L., Nakayasu, E.S., Oliveira, D.L., Nimrichter, L., Nosanchuk, J.D., Almeida, I.C., Casadevall, A., 2008. Extracellular vesicles produced by *Cryptococcus neoformans* contain protein components associated with virulence. Eukaryot. Cell 7. https://doi.org/10.1128/EC.00370-07.

Rodrigues, M.L., Nimrichter, L., Oliveira, D.L., Frases, S., Miranda, K., Zaragoza, O., Alvarez, M., Nakouzi, A., Feldmesser, M., Casadevall, A., 2007. Vesicular polysaccharide export in *Cryptococcus neoformans* is a eukaryotic solution to the problem of fungal trans-cell wall transport. Eukaryot. Cell 6. https://doi.org/10.1128/EC.00318-06.

Sabiiti, W., Robertson, E., Beale, M.A., Johnston, S.A., Brouwer, A.E., Loyse, A., Jarvis, J.N., Gilbert, A.S., Fisher, M.C., Harrison, T.S., May, R.C., Bicanic, T., 2014. Efficient phagocytosis and laccase activity affect the outcome of HIV-associated cryptococcosis. J. Clin. Invest. https://doi.org/10.1172/JCI72950.

Siqueira, L.P.M., Gimenes, V.M.F., de Freitas, R.S., Melhem, M.S.C., Bonfietti, L.X., da Silva, A.R.J., Souza Santos, L.B., Motta, A.L., Rossi, F., Benard, G., de Almeida, J.N.J., 2019. Evaluation of Vitek MS for differentiation of *Cryptococcus neoformans* and cryptococcus gattii genotypes. J. Clin. Microbiol. 57 e01282-18. https://doi.org/10.1128/JCM.01282-18.

Staib, F., 1962. *Cryptococcus neoformans* und Guizotia abyssinica (syn. G. oleifera D.C.). Z. Hyg. 148, 466–475.

Zaragoza, O., Rodrigues, M.L., De Jesus, M., Frases, S., Dadachova, E., Casadevall, A., 2009. Chapter 4 the capsule of the fungal pathogen *Cryptococcus neoformans*. Adv. Appl. Microbiol. https://doi.org/10.1016/S0065-2164(09)01204-0.